PHILOSOPHICAL TRANSACTIONS OF THE ROYAL SOCIETY A MATHEMATICAL, PHYSICAL & ENGINEERING SCIENCES

Displacement and Strain

J. G. Ramsay

Phil. Trans. R. Soc. Lond. A 1976 **283**, 3-25
doi: 10.1098/rsta.1976.0066

Phil. Trans. R. Soc. Lond. A. **283**, 3–25 (1976) [3]
Printed in Great Britain

Displacement and strain

By J. G. Ramsay, F.R.S.
Department of Earth Sciences, University of Leeds

The past decade has seen great advances in our knowledge of the finite strains in rocks deformed by natural tectonic processes. The current methods used in measuring strains are reviewed. These techniques rely on a knowledge of either lengths or relative lengths of lines before and after deformation, or of angles between line elements. Special techniques used in veined gneisses which have been used to assess the tectonics of Precambrian orogenic zones are discussed with regard to their validity in situations of volume dilation. The standard finite strain measurement techniques have now been extended to evaluate the sequence of progressive displacement and progressive strain in certain orogenic zones. Several types of regional strain patterns can now be recognized and these appear to be linked to differing tectonic environments.

Introduction

The concept of strain is a key one if we wish to understand the ordered rearrangements of the rock materials that take place in the crust of the earth during orogenesis. The basic mathematical principles were established by Cauchy (1828) and their application to the problems of deformed rocks was taken up by Philips (1843), Haughton (1856), Sharpe (1846), Sorby (1855), Heim (1878) and Daubree (1876). These geologists were quick to realize the importance of the strain ellipsoid theory and how it could be used to assess the significance of the linear and cleavage fabrics of deformed rocks. It was shown how the apparent multiplicity of fossil species of forms previously described from deformed rocks could often be reduced by an appreciation of the great variety of possible distortions of a single constantly shaped species when subjected to deformation. On a regional scale this led to the evaluation of strain variation over large sectors of orogenic zones (Cloos 1947) while the most recent developments of finite strain analysis on this scale have been attempts at integrating the strains over cross sections of fold belts in order to assess the amount of crustal shortening (Breddin 1964; Coward *et al.* 1976). Very complex finite strain variations occur in folded strata and over the past decade there has been a concerted attack on the mechanical problems of fold formation. In these studies, strain analysis has played a leading part and we have now come to the point where physical and computer modelling of the unstable processes leading to fold formation can be of real use to the practical geologist investigating the fold shapes of rock fabrics of naturally folded rocks. Some recent developments of the application of basic strain theory concern the general problems of progressive strain, how it may be possible to determine the evolutionary history of a deformed zone and relate the deformation history to temperature and pressure variations during deformation. Exciting new developments have been made possible by the use of electron microscopy and X-ray fabric techniques. Aided by chemical analysis of deformed rocks, we are beginning to be able to relate to the physical and chemical modifications of the crystals in the rock aggregate to the progressive strain history. A major rethinking of rock deformation in material terms is going on in structural geology similar to that which revolutionized the metallurgical sciences a few years ago.

The aim of this paper is to discuss the general principles of the strain theory with particular reference to any practical limitations of these principles when they are applied to geological problems. This will be followed by a review of the major techniques now employed to determine finite and progressive strain in naturally deformed rocks.

General theory of the relationships of displacement and strain

The study of displacement and the finite strains that may result from displacement is based entirely on the principles of three-dimensional geometry. It is independent of an analysis of the forces and stresses which lead to the movements and independent of any considerations of the dynamics of the processes relating stresses to strains.

The basic mathemtaical theory of strain is dependent on the idea that the body being deformed is, at the scale investigated, always a coherent, connected series of particles and that any displacements of one part of the body are constrained by the displacements of adjacent particles. This orderly displacement with the material acting as a continuum, enables mathematical relationships to be set up between the displacements and the internal distortions. As the principles of continuum mechanics are the basis of our analysis, it is worth considering the limitations of these principles to the types of displacements which go on in the rocks forming the crust. The ideas of orderly displacements imply that for any point with coordinates (x, y, z) in our undeformed body there exists only one final position in the displaced body with coordinates (x_1, y_1, z_1). This means that it is always possible to relate the final and initial points in the body by either of 2 sets of 3 displacement equations.

$$\left.\begin{aligned} x_1 &= F_1(x, y, z), \\ y_1 &= F_2(x, y, z), \\ z_1 &= F_3(x, y, z). \end{aligned}\right\} \tag{1}$$

$$\left.\begin{aligned} x &= F_4(x_1, y_1, z_1), \\ y &= F_5(x_1, y_1, z_1), \\ z &= F_6(x_1, y_1, z_1). \end{aligned}\right\} \tag{2}$$

The first set is known as a *Lagrangian description* of the displacements, and relates the positions of the deformed points in terms of functions of the initial positions of those points, whereas the second set is known as an *Eulerian description* and describes initial positions in terms of final positions of those points. The two sets of equations describe the same displacement; both sets are useful for the analysis of geological problems, the first set is most convenient for an analysis of the development of strain, the second set is most convenient for an investigation of strain in deformed bodies (see Ramsay & Graham 1970). In both sets of equations the functions F_1, etc., are continuous single valued functions over all real values of x, y and z.

The general result of such a continuous deformation, where the functions F are nonlinear, is to produce a displacement and heterogeneous distortion throughout the body (figure 1). Any originally orthogonal grids drawn on the undeformed material become curved, and any identical shaped initial elements take up different shapes in the deformed state. If we focus our attention on a very small element in the body and observe the changes of shape of a square and

circle (in 2 dimensions) or a cube and sphere (in 3 dimensions) drawn on the undeformed material we find that these are transformed to a parallelogram, ellipse, parallelopiped and ellipsoid respectively. These shape changes can be used to define the state of strain (s) at that point. The geometric modifications which are used to define strain change smoothly from point to point in the body, and strain variation in any direction can be expressed as a continuous function of initial or final coordinates.

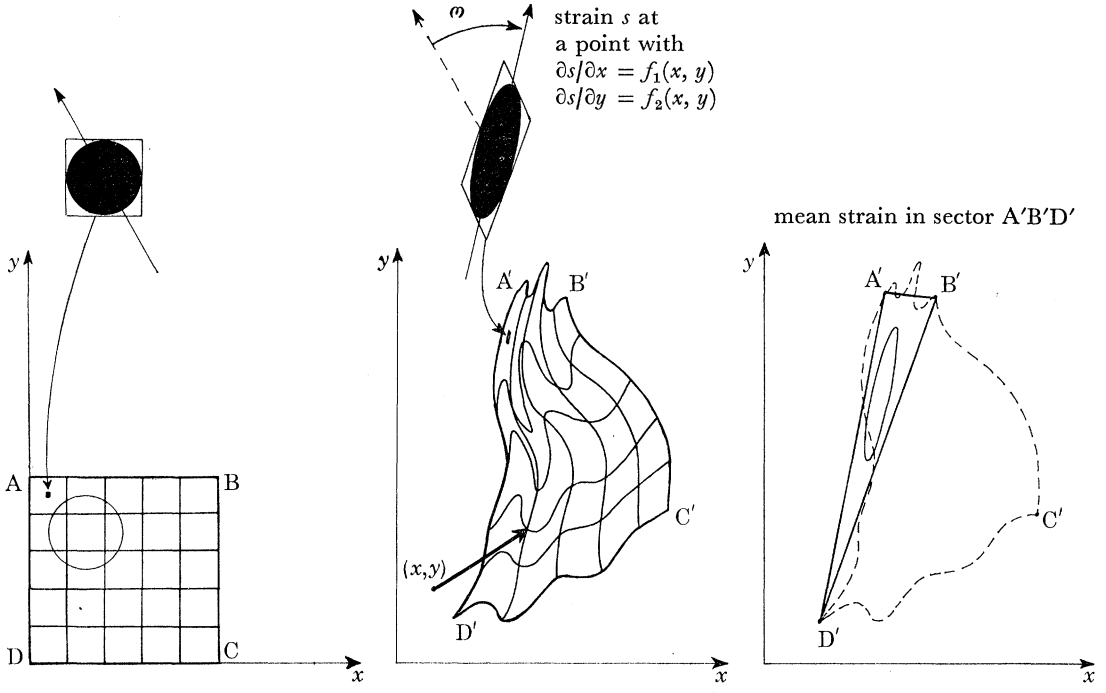

FIGURE 1. The geometric principles of displacement and strain in two dimensions.

The state of strain at a point can be analysed in terms of components. In two dimensions (figure 1) four terms are used to specify the local displacements around the point (known as the displacement gradients) and the state of strain is also specified by four components. These are (1 and 2) the values of a maximum and minimum elongation, (3) the orientation of the maximum elongation and (4) the amount of body rotation ω undergone by the line which has become the direction of maximum elongation. The geometrical effects of strain are most effectively visualized by considering the geometric changes undergone by an initial circle with unit radius. This is transformed to an ellipse, the *strain ellipse*, whose major and minor semi-axes define the principal strains, and the orientation and rotation of its long axis define the third and fourth terms. In three dimensions nine terms are required to specify the local displacement gradients and nine terms are required to describe completely the state of strain at a point. These nine terms are best visualized by considering the geometric modifications of an initial unit sphere which is transformed to an ellipsoid. The *strain ellipsoid* has three components defining the lengths of its mutually perpendicular semi-axes ($1+e_1$, $1+e_2$ and $1+e_3$) where the three principal strains are e_1, e_2 and e_3, three defining the orientation in space of three axes X, Y and Z of e_1, e_2 and e_3 respectively and three describing the rotations made by these three

directions from their initial directions in the sphere. The mathematical relationships between the displacement functions and the various principal strain parameters will not be described here. They can be found in Ramsay & Graham (1970).

The concept of homogeneous strain can only be applied at a single point in a heterogeneously deformed body. In geological problems, particularly those connected with large scale regional distortions, it is sometimes useful to consider the average strain or *mean strain* through a large volume of rock (figure 1). If we consider a triangular element ABD in the initially undeformed body, then this will be distorted into some other triangular element A′B′D′. The mean strain refers to the distortional changes which have taken place in this whole sector as reflected in the strain ellipse shown in figure 1*c*. There is no simple way of describing the mean strain in terms of individual observations of finite strain at several points in the sector. The mean strain state can only be assessed by integrating the local displacements set up by the local strains to compute the total displacement gradient over the sector A′B′D′.

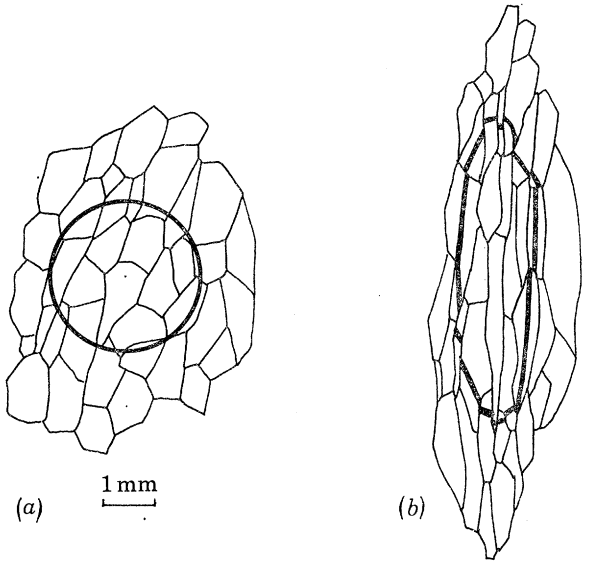

FIGURE 2. The limitations of the principles of continuum mechanics in a polycrystalline aggregate. The initial circle in the undeformed aggregate (*a*) will not take up the form of a perfect ellipse in the deformed material (*b*).

Limitations

The main limitations in the application of this theory to the study of rock deformation concerns the scale of our observations. The concept of homogeneous finite strain in a heterogeneously strained body is a mathematical idea only correct at a single point in the body. The strain ellipsoid concept can therefore only be applied to a piece of rock which has a size small enough for the strains to be effectively homogeneous. One method of testing this is to seek sets of planes which were parallel before deformation and which remain parallel after deformation. The most obvious set of natural planar markers are bedding or lithological layering.

A second important limitation is that most natural deformations are not continuous. The theory is not applicable where there are faults, holes, chaotic mixing or the removal of certain parts of the body. It is well known that faults and spaces do occur in naturally deformed rocks, and although the processes of chaotic mixing are less common, local removal of certain parts of the rock during the process known as pressure solution is well known. All these types of

discontinuity limit the direct application of the mathematical theory, but the predictions still apply to the rock material in the domains between the discontinuities.

Another limitation to the continuum mechanics principles concerns the scale at which we make our observations. Rocks are polycrystalline aggregates of minerals, generally of several species of mineral. During deformation, each grain undergoes its own special type of modification depending on its orientation, plasticity and chemical stability under the specific temperature and pressure conditions during deformation. Adjacent grains may remain in contact, they may slide one against the other, or undergo some local solution or addition of new material along their contacts. It will be clear that when we observe the rock material at a scale where we can observe the individual grains, the principles of continuum mechanics will not apply. A circle drawn on a surface of the undeformed crystal aggregate (figure 2) will not be deformed into a perfect ellipse, although the statistical average of the component parts will approximate to an elliptical form. For the mathematical theory of the continuum mechanics approach to have some direct application to rocks we have to make our observations at a scale that will smooth out the discontinuities that occur at the crystalline scale. In practice this is no great restriction to the application of the theory in the field as most hand specimens of rock contain a sufficiently large number of crystals for the intercrystalline discordances to be negligible. However, when we begin to relate the internal deformation mechanisms of individual crystals in an aggregate to the average strain of the whole rock we must be aware of this problem.

Strain measurement

The basis of all strain determination in naturally deformed rock is to make measurements on embedded objects of which something is known about their initial shape or size. If the embedded objects have an appreciable volume, an accurate strain analysis will only be made if they are of the same composition as their enclosing matrix, so that the ductility contrasts are minimal.

A complete specification of all nine components of the strain state at any one point is generally impossible. The three rotational components are the most difficult to measure, because having only deformed material we can only assess the final and not the initial orientation. With certain types of embedded markers it is possible to define completely the three principal strains and their orientations; that is the other six strain components. With many of the markers used for strain analysis, however, only the proportional ratio of the principal strains can be established.

Practical strain analysis generally proceeds by making two or preferably three two dimensional strain determinations and then combining these to form a complete picture of the three dimensional strain state. It is usual to try and make these two dimensional determinations on the three principal planes XY, XZ and YZ, but solutions can be found on any three perpendicular planes (Ramsay 1967, pp. 142–147) and are even possible with any three non-parallel planes (Ramsay 1967, pp. 147–148). As might be expected, the mathematical analysis is easiest if one uses the principal planes, and heaviest if one uses any three non-parallel planes. The advantage of these methods is that one has recourse to internal checks on the accuracy of the individual determinations (Ramsay 1967, pp. 199–200) and to calculate the errors (Roberts & Siddans 1971).

PHILOSOPHICAL TRANSACTIONS OF THE ROYAL SOCIETY A MATHEMATICAL, PHYSICAL & ENGINEERING SCIENCES

Initially spherical or circular objects

Objects of this type generally offer ideal material for determining the strain ellipsoid, providing that there is no marked competence contrast between the object and its matrix. The techniques for recording and analysing this data are well documented (Cloos 1947; Ramsay 1967). A mathematically related problem concerns the rearrangement of initially equally distributed points in space as a result of strain. The type of problem that can be solved in this way is the change in distribution of the node-like meeting points of polygonal cells in a polygonally jointed igneous rock. In the undeformed state the wall length distance between any two nodal points should not show any significant variation with orientation, but on deformation they will be distorted in direct proportion to the lengths of the diameters of the strain ellipse. An analysis of these changes of lengths using the techniques described by Ramsay (1967, pp. 195–197) will enable the orientation and strains to be determined. A word of warning should be put in here about the applicability of this method to the analysis of strain in any randomly distributed series of points. If the nearest neighbour lines of the undeformed aggregate can be established, then this technique can be used; but if they cannot be established then the method is inapplicable. The reason is that any deformed randomly distributed aggregate of points produces a reoriented array which is also randomly distributed, and from the final array it is impossible to tell which direction has been 'stretched' and which has been contracted.

Initially ellipsoidal or elliptical objects

Nature has rarely presented us with perfectly spherical embedded markers in undeformed rocks, and most oolites, vesicles, conglomerate pebbles, reduction spots, etc., have an initially sub-ellipsoidal form. This initial shape factor has sometimes been ignored but this is most unwise because the shape of any deformed initially elliptical objects contains an inherited shape factor which enters as a matrix product into the final shape. The initial shape is not diluted by the distortional factors no matter how large these factors are.

There are now a well documented series of mathematical techniques for the analysis of randomly oriented initially elliptical aggregates of the types shown in figure 3 (Ramsay 1967, pp. 202–216; Dunnet 1969; Elliott 1970; Matthews *et al.* 1974). Situations where there is a statistically preferred orientation of the initial ellipses such as is shown in figure 3 can now be resolved into their tectonic and original components (Ramsay 1967, pp. 216–271; Dunnet & Siddans 1971, Roberts & Siddans 1971), and computer programs are available to make the somewhat tedious mathematical procedures a practical reality.

Perhaps the most acute problem with strain determination of spherical and ellipsoidal objects concerns the difference in ductility between the object and its matrix (Gay 1968, 1969). This is a formidable problem the solution to which is still under debate (see the discussion following Gay & Fripp's paper in this volume, p. 125).

Line strain gauges

In engineering technology strains are commonly analysed by attaching electrical resistance strain gauges on the surfaces undergoing deformation and using these to compute changes in length. In the natural deformation of rock materials, we occasionally have embedded in the rock objects from which linear extensions can be determined. Crinoid stems and belemnites have been used most frequently as line strain gauges (Daubrée 1876; Heim 1878, 1919; Brace

PHILOSOPHICAL TRANSACTIONS OF THE ROYAL SOCIETY A MATHEMATICAL, PHYSICAL & ENGINEERING SCIENCES

1960; Badoux 1963; Ramsay 1967). With any three differently oriented line elements it is possible to establish three equations which may be solved for the two principal quadratic extensions ($\lambda_1' = 1/(1+e_1)^2$, $\lambda_2' = 1/(1+e_2)^2$) and the orientation of these axes (θ') (figure 4). It should be noted that these three equations are more elaborate than those used by engineers investigating small or elastic infinitesimal strains and which ignore the second order terms arising by the products and powers of small terms. The finite strain equations can be solved

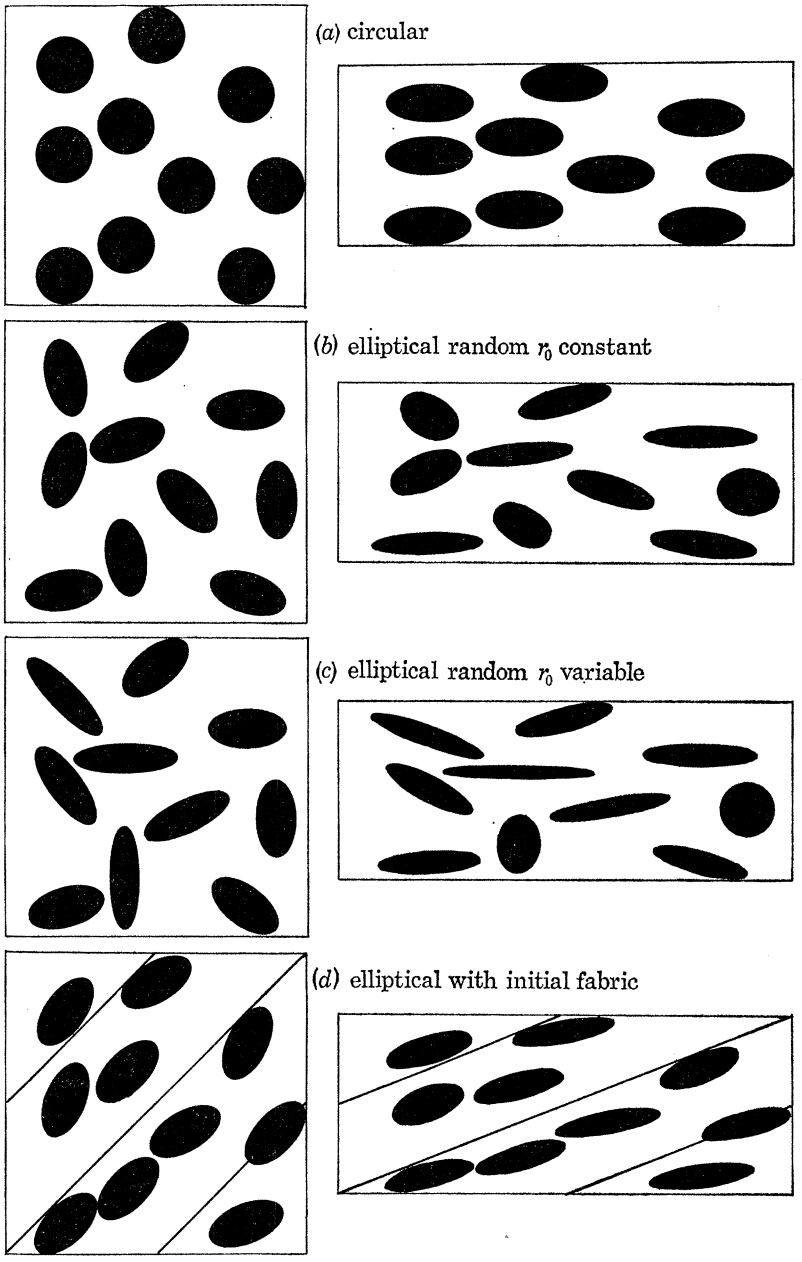

FIGURE 3. The deformation of initially circular and elliptical markers by homogeneous strain. Circular markers deform into a series of identically shaped ellipses (*a*), whereas elliptical markers take up a range of final elliptical shapes depending upon their initial shapes (ellipticity ratio r_0) and orientations and the degree of initial preferred alignment (*b*, *c* and *d*).

PHILOSOPHICAL TRANSACTIONS OF THE ROYAL SOCIETY A MATHEMATICAL, PHYSICAL & ENGINEERING SCIENCES

numerically but they can also be evaluated very rapidly using the graphical method known as Mohr construction (Brace 1960, 1961; Ramsay 1967, pp. 79–81).

Angle strain gauges

Certain features of objects contained in rocks can be used for an analysis of strain by means of assessing the significance of angular changes. Initial perpendicular relations between lines and planes are fairly common, for example, bilaterally symmetric fossils, mud cracks and bedding surfaces, scolithus tubes penetrating through bedding planes, cooling joints at the walls of intrusions. Nature also provides a number of other fixed angular relations, for example, regular pentagonal symmetry is found in certain crinoids, hexagonal symmetry in certain corals, and in a crude form in arrays of polygonal cooling joints or dessication cracks. More complex but regular angular relations may be found in the spirals of gastropods and the regular logarithmic growth spirals of ammonites. The basic numerical analysis is developed by consideration of the modifications of initially perpendicular lines during strain. The deflexion of the lines away from their initial state of perpendicularity is known as the angular shear strain (ψ). This can always be expressed in terms of the principal strain ratios and the orientation of one of the lines with the principal strain (θ', figure 5). It therefore follows that any two measurements of angular shearing strain in a deformed surface are sufficient to calculate the two principal features of the strain state by numerical or graphical solution of the equations (Ramsay 1967,

$$\lambda'_A = \lambda'_1 \cos^2 \theta' + \lambda'_2 \sin^2 \theta'$$

$$\lambda'_B = \lambda'_1 \cos^2 (p - \theta') + \lambda'_2 \sin^2 (p - \theta')$$

$$\lambda'_C = \lambda'_1 \cos^2 (q - \theta') + \lambda'_2 \sin^2 (q - \theta')$$

for 3 unknowns $\lambda'_1 \lambda'_2 \theta'$

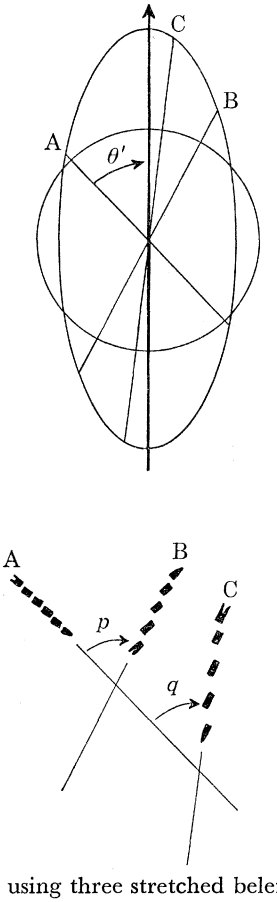

FIGURE 4. The techniques for using three stretched belemnites as linear strain gauges to determine the strain ellipse.

pp. 76–78; 230–243). The more complicated angular relations of pentagons and hexagons can easily be resolved into a series of mutually perpendicular initial relations. For example, constructions such as those shown in the deformed pentacrinus ossicle illustrated in figure 6 enable five separate determinations of the angular shear strain for a single fossil – clearly this particular problem is over defined. More complex angles such as those found in irregular molusca can also be resolved to compute the angular shearing strains necesary to establish the basic equations (Ramsay 1967, pp. 243–246) and Tan (1973) has shown how even small fragments of deformed ammonites can be used to determine the principal features of the strain.

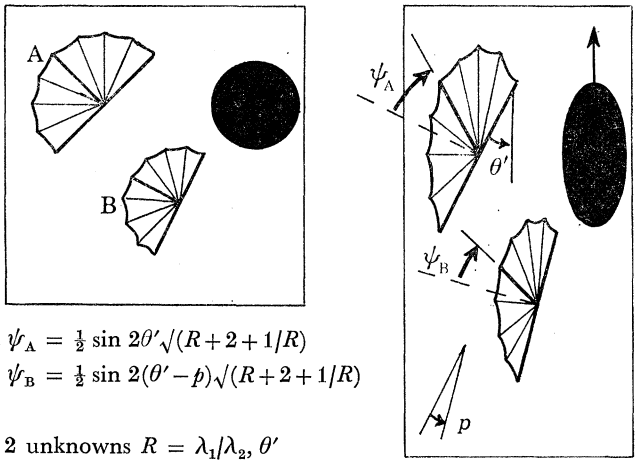

FIGURE 5. The use of angular shear strain (ψ) measurements in two deformed brachiopods to determine the strain.

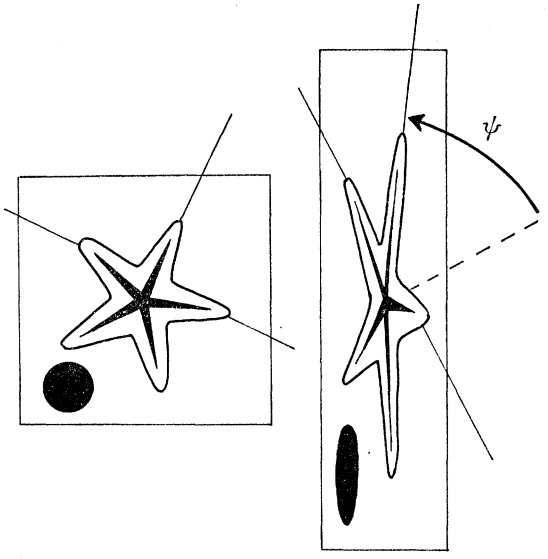

FIGURE 6. Method of computing angular shear strain in a pentacrinus ossicle.

As a result of strain, all line elements deforming homogeneously with their enclosing rock, become redistributed so that in the deformed state there will be a clustering around the direction of the greatest elongation. This well documented effect has been used to explain how certain crystals become realigned in deformed rocks, a process which can lead to the development

of planar and linear fabrics (March 1932; Owens 1973). This reorientation of non-rigid line elements is controlled by the rigid body rotation (the same for all initial orientations) together with an effect which leads to a reduction in initial angle θ the line makes with the direction which becomes the maximum extension to a value θ' such that

$$\tan\theta' = \tan\theta' (1+e_2)/(1+e_1)$$

(figure 7). This rearrangement can lead to striking reorganization of initially random distributions into markedly preferred orientations even at comparatively low strains (figure 8). After deformation, the ratio of those linear elements distributed around the maximum extension to

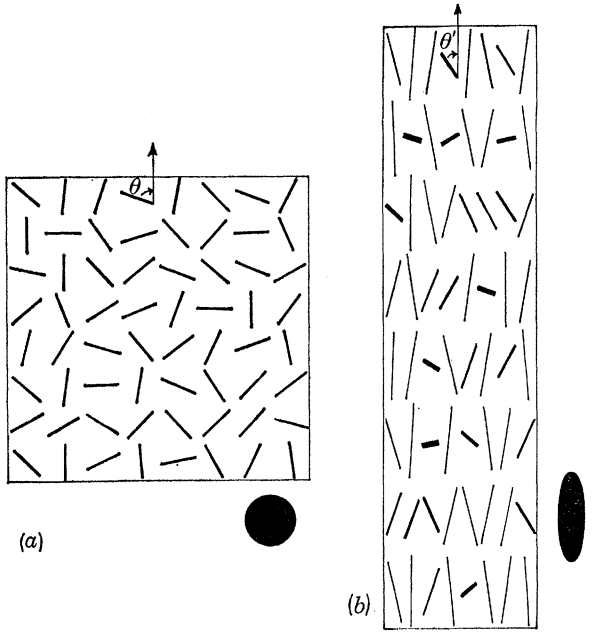

FIGURE 7. Rearrangement of uniformly distributed line elements (*a*) as a result of homogeneous strain (*b*).

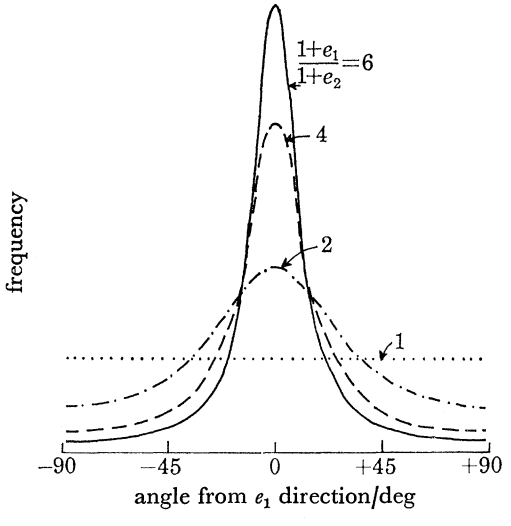

FIGURE 8. Frequency of line element orientations resulting from strain of an initially randomly oriented array.

PHILOSOPHICAL TRANSACTIONS OF THE ROYAL SOCIETY A MATHEMATICAL, PHYSICAL & ENGINEERING SCIENCES

those around the minimum extension direction is a function of the square of the principal strain ratios. This analysis of the degree of preferred orientation of initially randomly distributed lines (for example, the traces of the browsing trails of marine organisms on a bedded surface) gives an excellent method for determining the strain ratios on that surface.

Techniques of strain analysis in gneissic rocks

In many rocks the techniques for strain determination described above are not applicable because suitable objects of known original shape or size are unavailable. Many areas of the exposed crustal surface consist of Precambrian banded gneissic rocks probably representing once deep seated parts of the crust brought to the surface by later tectonic events and unroofed by erosion. Although these rocks are generally intractable to strain analysis by many of the techniques described above the idea for a potentially very powerful method was proposed by Flinn

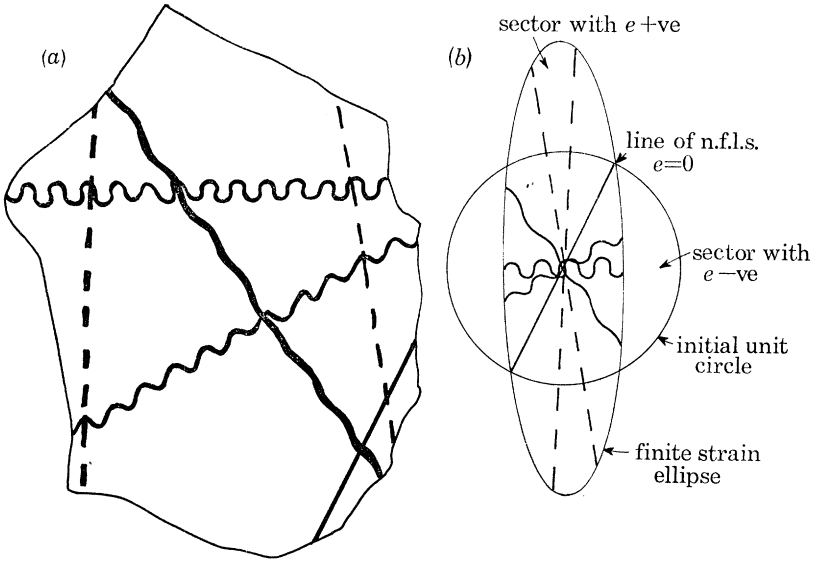

Figure 9. Deformation of competent veins by boudinage and folding, and the relations of these structural styles to the directions of no finite longitudinal strain (n.f.l.s.) in the strain ellipse.

(1962) and worked out in some detail by Talbot (1970). The basic technique of this method is to determine the orientations of lines of no finite longitudinal strain ($\lambda = 1$) in the body of rock under examination and then to use this information to construct the shape and orientation of the surface of no finite longitudinal strain contained in the strain ellipsoid. The method requires that the rock contains a number of variably oriented competent layers surrounded by a less competent host material, so that when the rock mass as a whole is deformed, the competent layers are subjected to a finite contraction and are buckled, or are subjected to an elongation and are boudinaged (figure 9). If the competent layers (such as the veins and dykes of aplite and pegmatite so common in granite gneisses) had a number of different initial orientations it should be possible to determine the orientation of lines separating the buckle fold and boudinage fields – the full details of the technique are described in Talbot (1970, pp. 49–54). Finite strain

ellipsoids can be divided into five major types depending on the values of the prinicpal strain values:

(1) $\lambda_1 > \lambda_2 > \lambda_3 > 1$
(2) $\lambda_1 > \lambda_2 > 1 > \lambda_3$ true flattening type ellipsoid
(3) $\lambda_1 > \lambda_2 = 1 > \lambda_3$ plane strain ellipsoid
(4) $\lambda_1 > 1 > \lambda_2 > \lambda_3$ true constrictional type ellipsoid
(5) $1 > \lambda_1 > \lambda_2 > \lambda_3$

Types 1 and 5 are unlikely to occur as a result of natural geological deformation because they involve extreme volume increase (type 1 where all dimensions of the initial unit sphere are elongated) or extreme volume decrease (type 5 where all dimensions are contracted).

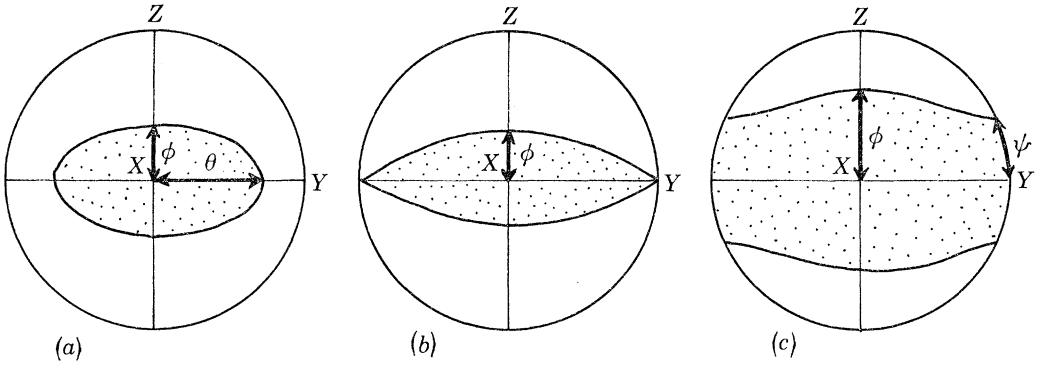

FIGURE 10. Constrictional (*a*), plane strain (*b*), and flattening (*c*) ellipsoids in equal area projection showing the angles used to define the surface of no finite longitudinal strain separating extended directions (stippled) from contracted directions (unstippled). *X*, *Y* and *Z* are the principal strain directions.

Tectonic deformations will always be of types 2, 3 and 4 and all of these can show volume changes or dilations which can be positive, zero or negative. The special ellipsoid types 1 and 5 have no directions of no finite longitudinal strain, lying either completely outside or completely inside the unit sphere from which they were derived. Ellipsoid types 2, 3 and 4 all have directions of no finite longitudinal strain arranged on conic surfaces. The lines of no finite longitudinal strain arising from the intersection of the strain ellipsoids of type 2 and 4 and the initial unit sphere are generally arranged on an elliptical cone. This form degenerates to two crossing planes (circular sections) in the special type of plane strain ellipsoid type 3. These surfaces of no finite longitudinal strain can be specified by making angular measurements of the intersections of the surfaces of no finite longitudinal strain on two of the *XY*, *YZ* or *ZX* principal planes (table 1, figure 10).

TABLE 1

	XY	*XZ*	*YZ*
oblate type 2	no intersection	ϕ	ψ
type 3	parallel to y	ϕ	parallel to y
prolate type 4	θ	ϕ	no intersection

Talbot has shown that if there has been no volume change, it is possible to derive the three principal strains from the angles defining the surfaces of no finite longitudinal strain (Talbot 1970, pp. 59–65). As deformation generally takes place with some volume change, the utility of this interesting and valuable technique will now be examined to see what constraints are imposed if volume changes do occur.

With flattening ellipsoids (type 2) the angles ϕ and ψ may be expressed in terms of the reciprocal principal strains on the principal plane sections ($\lambda_1' = 1/\lambda_1$, λ_2' and λ_3') (Ramsay 1967, p. 66)

$$\tan^2\phi = \frac{1-\lambda_1'}{\lambda_3'-1}, \tag{3}$$

$$\tan^2\psi = \frac{1-\lambda_2'}{\lambda_3'-1}. \tag{4}$$

The relations of the principal strains and the volume change Δ is given by

$$\lambda_1'\,\lambda_2'\,\lambda_3' = 1/(1-\Delta)^2. \tag{5}$$

Combining these three equations to solve for λ_3' we obtain a cubic

$$\lambda_3'^3 - \lambda_3'^2(2+\cot^2\psi+\cot^2\phi) + \lambda_3(1+\cot^2\psi+\cot^2\phi+\cot^2\psi\cot^2\phi)\frac{-\cot^2\psi\cot^2\phi}{(1+\Delta)^2} = 0$$

which may be factorized

$$[\lambda_3'-1]\,[\lambda_3'^2-\lambda_3'(1+\cot^2\psi+\cot^2\phi)+\cot^2\psi\cot^2\phi] = \cot^2\psi\cot^2\phi[1/(1+\Delta)^2-1]. \tag{6}$$

The nature of the three roots depends on the numerical value taken by the right hand side of (6). If there is no change in volume ($\Delta = 0$) there are three real roots given by

$$\lambda_3' = 1, \tag{7a}$$

$$2\lambda_3' = 1+\cot^2\psi+\cot^2\phi+[(1+\cot^2\psi+\cot^2\phi)^2-4\cot^2\psi\cot^2\phi]^{\frac{1}{2}}, \tag{7b}$$

$$2\lambda_3' = 1+\cot^2\psi+\cot^2\phi-[(1+\cot^2\psi+\cot^2\phi)^2-4\cot^2\psi\cot^2\phi]^{\frac{1}{2}}. \tag{7c}$$

The first of these has no relevance to deformed materials, for it relates to the unstrained unit circle ($\lambda_1' = \lambda_2' = \lambda_3' = 1$). Of the other two roots, the second will be found to give negative values for λ_2' and λ_3' and as these must be positive quantities to satisfy the real geometry it produces imaginary mathematical root quantities which have no geological significance. The third root substituted in 1 and 2 gives real positive values for both λ_2' and λ_1' and is the unique geological solution to the problem. It is the same as that derived by Talbot (1970, p. 60) although expressed in different terms. The advantage of the method discussed above over Talbot's is that it enables the problem to be solved where volume change does occur.

The effect of volume change is to give real positive value (where Δ is $-$ve) or real negative value (Δ +ve) to the right hand side of (6). Volume change does not alter the nature of the variables of the left hand side of (6). To consider the effect of this, figure 11*a* illustrates the cubic function expressed for an ordinate value of $\Delta = 0$, for all oblate ellipsoids with $\phi = 18.10°$ and $\psi = 14.96°$. Any point on this graph will give a mathematically correct solution to (6), but only those marked on the continuous part of the curve have significance to geological problems. We have seen how the solution to the ellipsoid is unique if there is no volume change, however, *two real solutions* are possible if there is volume reduction. For example with a 20 % volume loss solutions to (6) are found in figure 11*c* along a line cutting the curve given by

$$y = \cot^2\psi\cot^2\phi\,(1/(1+\Delta)^2-1) = 73.47.$$

This cuts the cubic at three points, two giving real solutions to λ_3', λ_2' and λ_1' and one which gives imaginary solutions λ_2' and λ_1'. The problem is therefore *not uniquely soluble* unless additional information is available on the shape of the strain ellipsoid. In practice this additional data

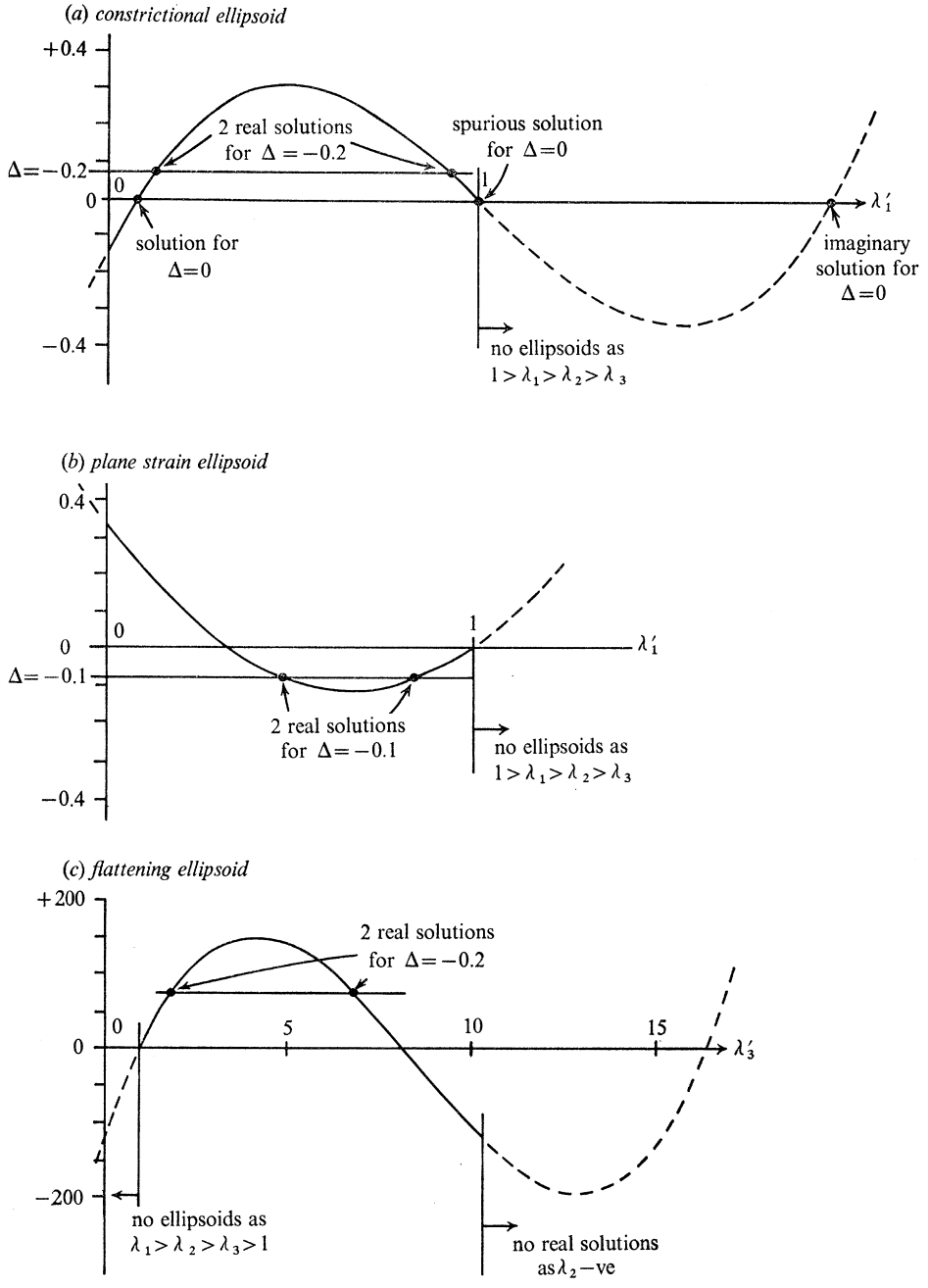

FIGURE 11. Different types of solutions to the values of the principal strains derived from surfaces of no finite longitudinal strain. Real solutions are found along the continuous sectors of the curves, and solutions of no geological significance are located on the dashed curves.

could be information about the strain ratios derived from embedded objects. Since the whole point of this type of analysis is to tackle situations where data about the strain ratio derived from objects are not available, it might be more practical to choose the most likely root by examination of the intensity of the deformation from the intensity of rock fabric or tightness of buckle folds. In some instances it might be possible to choose the most likely root by examination of

the type of rock fabric – whether linear (l) or planar (s) or mixed (ls), matching the fabric to the differing k value of the two ellipsoids $k = (\lambda_1 \lambda_3)^{\frac{1}{2}}/\lambda_2$.

It will be clear from this discussion that a whole range of ellipsoids can have the same surface of no finite longitudinal strain. The ranges of ellipsoids satisfying $\psi = 14.96$ and $\phi = 18.10$ are indicated in a strain ratio plot in figure 12, together with their volume changes and values of total shortening along the Z direction. The ellipsoids which are true flattening ellipsoids with $\lambda_2 > 1$ mostly plot in the apparent flattening field of oblate shape, yet some do occupy the prolate shape field. This graph can also be used to assess the size of errors in percentage shortening calculated along the Z (λ_3) direction if volume changes cannot be determined. Volume changes clearly cannot be ignored if strain determinations are required to a high accuracy. Although volume losses may be quite large in certain types of deformed sediments (Ramsay & Wood 1973), very little is known about the extent of volume changes in gneissic basement rocks.

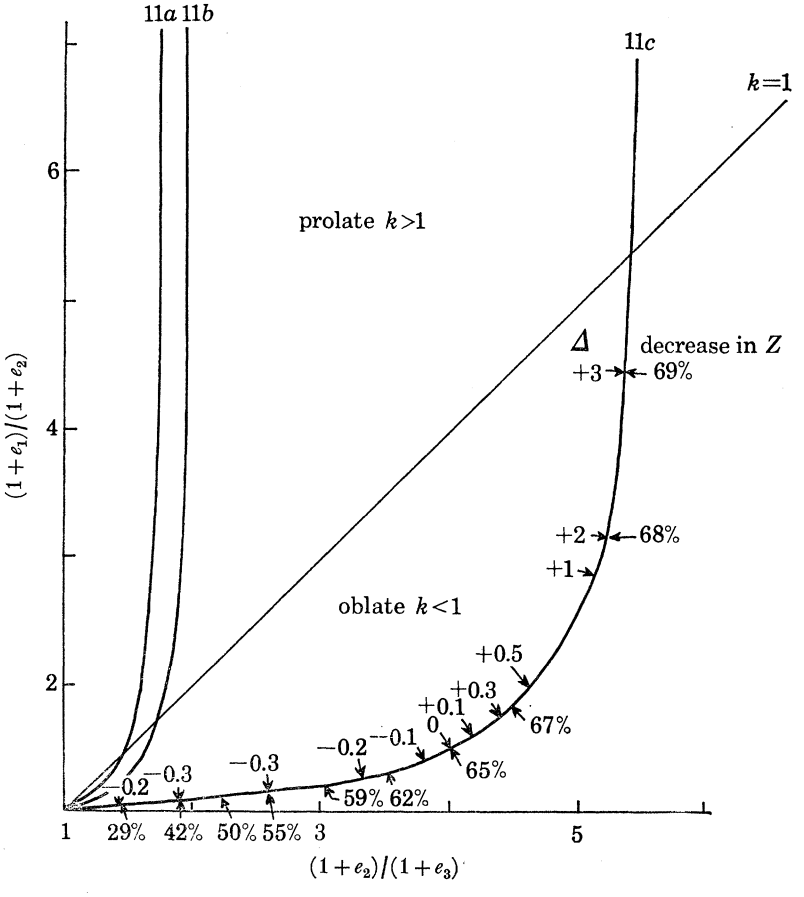

FIGURE 12. Plots of all possible ellipsoids shown in figure 11.

Although gneisses are unlikely to lose appreciable volume by closing up of intergranular voids, metamorphic changes commonly lead to dehydration, and the fluid which leaves the rock system could be responsible for removing more soluble rock components in solution. Barr & Coward (1974) have combined a strain analysis by the deformation of lines of no finite longitudinal strain with strain ratio measurements in Archaean volcanics from the greenstone belts of Rhodesia and Botswana and have shown volume range of $\Delta = +0.04$ to -0.115. In

gneissic terrain there is a further possibility that migmatization may lead to the influx of solid and hydrous components into the rock and this could give rise to a significant volume increase. Quite apart from the regional implications of strain measurements to determine large scale crustal displacements and deformation during orogenesis, it is clearly useful to evaluate distortion and volume change effects to assist an understanding of the significance of the actual chemical processes going on during deformation.

With plane strain (type 3) ellipsoids the principal strains are determined by combining the equations for ϕ with those for volume change

$$\tan^2\phi = \frac{1-\lambda_1'}{\lambda_3'-1} \quad \text{and} \quad \lambda_1'\lambda_3' = 1/(1+\Delta)^2$$

to give

$$(\lambda_1'-1)\,(\lambda_1'-\tan^2\phi) = \tan^2\phi\,[1-1/(1+\Delta)^2]. \tag{8}$$

This quadratic in λ_1' has two roots. If there is no volume change one of these is of spurious significance ($\lambda_1' = 1$) and there is a unique solution given by $\lambda_1' = \tan^2\phi$. With a volume reduction two real roots may be possible depending on the nature of the intersection of the line $y = \tan^2\phi\,(1-1/(1+\Delta)^2$ with the parabola. An indication of the possibilities is shown in figure 11*b* where $\phi = 30°$. Resolution of this double solution to the problem has to be tackled by some other means as discussed above. As with the type 4 ellipsoid described above there is a great range of possible finite plane strain ellipsoids with $\phi = 30°$ with a variety of volume changes and values of maximum shortening. The shape spectrum is shown in figure 12; some plot in the oblate shape field, some in the prolate field. As previously pointed out (Ramsay 1967, p. 162; Ramsay & Wood 1973) only those which have zero volume change lie on the $k = 1$ line.

The remaining type of ellipsoid (type 4) showing lines of no finite longitudinal strain arranged in a conical form is that of the true constrictional type. The determination of the principal strain from the two angles θ and ϕ defining the surface of no finite longitudinal strain follows identical methods to those employed for type 2 ellipsoids leading to a cubic equation for values of λ_1':

$$[\lambda_1'-1]\,[\lambda_1'^2-\lambda_1'(1+\tan^2\phi+\tan^2\theta)+\tan^2\phi\,\tan^2\theta] = \tan^2\phi\,\tan^2\theta\,[1/(1+\Delta)^2-1]. \tag{9}$$

Solutions to this proceed in exactly the same way as those for oblate ellipsoids. Where there is no volume change there is one geologically significant root given by:

$$2\lambda_1 = 1+\tan^2\theta+\tan^2\phi-[(1+\tan^2\theta+\tan^2\phi)^2-4\,\tan^2\theta\,\tan^2\phi]^{\frac{1}{2}}. \tag{10}$$

Where a volume loss has occurred, of the three valid mathematical solutions to (9), only two are geologically valid. These two can only be resolved by bringing in some other data. A typical case of this type with $\theta = 42.50°$ and $\phi = 22.40°$ is shown in figure 11*a*, with solutions for $\Delta = 0$ and $\Delta = -0.2$ and the whole spectrum of possible ellipsoid shapes having the same θ and ϕ values as shown in figure 12.

Strain increment measurement

The techniques so far discussed are methods for computing the total rock strain irrespective of how the finite strain has been built up. Straining is clearly a progressive process and the wide range of possibilities that can arise during the process of progressive deformation were first pointed out by Flinn (1962). Although the process of deformation is a continuous one it is

sometimes geometrically and geologically convenient to analyse it in a series of incremental stages. This means that at any one time during a deformation sequence, it is possible to consider the effects of small incremental distortion and rotation of infinitesimal dimensions superimposed on an already established finite strain state (Ramsay 1967, p. 114; Durney & Ramsay 1973). The implications of the general non-parallelism of the increment distortion principal strains to the finite principal strains on the development of structures in the rock are very considerable. Flinn (1962) was the first to point out how, under certain circumstances, previously folded competent layers might be unfolded later during the same deformation and Ramsay (1967, pp. 114–174) described in more general terms the effects of this superimposition.

The concepts of progressive deformation are particularly important in interpreting tectonic evolution of an area. Several workers have independently realized that it might be possible to evaluate the orientations and values of the progressive strain increments by study of the morphological forms of certain crystals which grow at the same time as the deformation. Wickham and Elliott (1970), Elliott (1972), Durney & Ramsay (1973), have all described the fibrous crystal fillings that are commonly found in so called pressure shadow zones, attributing their fibrous forms to preferential progressive growth at one end of the crystal during a deformation sequence. Durney & Ramsay (1973) have also extended their analysis to include various types of fibrous crystal filling found in tensile fissures and along fault surfaces and have devised techniques by which the incremental strains acting in a certain direction can be measured. The actual method depends on the nature of the system, and on which end of the fibrous crystal additions of new material are taking place. Figure 13 illustrates the type of fibrous quartz growth commonly found in the pressure shadow zones around sub-spherical masses of framboidal pyrite. During deformation the matrix is progressively pulled away from the surface of the pyrite along the direction of the greatest principal incremental extension, and the potential space is continuously filled with new crystallizing quartz (generally attached to quartz crystals in the detached matrix wall of the pressure shadow zone). Progressive addition to the quartz crystals always takes place on the quartz and pyrite interface and the crystals acquire a fibrous form with the directions of the fibres being parallel to the direction of the incremental extension at the time of the silica addition. Changes in the principal incremental strain direction leads to curving fibres of quartz which are in uniform optical continuity throughout. The process is schematically represented in figure 13 for three differently oriented and differently valued strain increments. If the incremental strain directions change suddenly the bends in the crystal fibres are very marked, whereas if more continuous changes occur the crystals in the fibres are smoothly curved. By making measurements of the lengths of fibres in a certain direction and comparing these to the diameters of the pyrite sphere it is possible to determine the incremental strain in specific directions (figure 14), and produce graphs of the changing directional increments with time. This technique has been applied to certain nappe zones in the Helvetic Alps of Switzerland (Durney & Ramsay 1973). It has been shown that the deformation histories of different nappes vary considerably and can in part be related to the vertical tectonic position in the nappe pile. The upper nappes in the pile show very variable deformation sequences probably because they were close to the surface. The lower nappes evolved at a later stage, carrying the upper nappes in piggy-back fashion and undergoing a more regular progressive deformation being constrained by the presence of the overlying nappes and confined from the sides by the presence of other rock material.

PHILOSOPHICAL TRANSACTIONS OF THE ROYAL SOCIETY A MATHEMATICAL, PHYSICAL & ENGINEERING SCIENCES

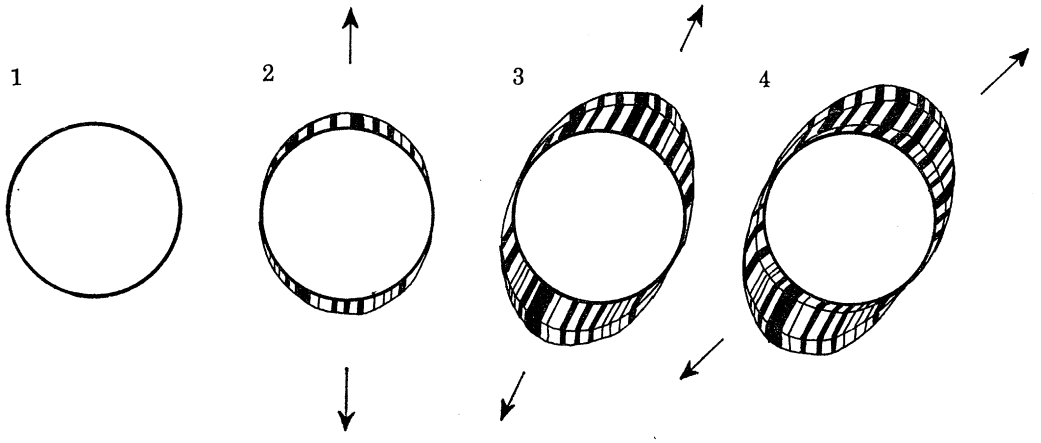

FIGURE 13. The shapes of fibrous crystals growing in pressure shadow zones, and the relations of the fibre lengths to the incremental extensions.

LARGE SCALE STRAIN PATTERNS

Several types of patterns of strain variations in constricted crustal rocks have become apparent regional strain investigations. The different types of strain distributions appear to be controlled by the following factors:

1. *Rock anisotropy*. A rock may be anisotropic or nearly so. It may possess a marked physical layering or have some pervading planar or linear fabrics which are important in controlling the types of instability produced during deformation.

2. *The amount of fluid contained in the rock and the pore pressure of the fluid*. Increases in pore pressure produce very striking effects dependent on the permeability of the rock and the strain rate during deformation. At high strain rates and low permeability, high pore pressure approaching that of the lithostatic load, can build up.

3. *The ductility of the rock material*. Rock ductility depends on the temperature and confining pressure (factors which both increase more or less systematically with depth) and on the strain rate and internal fluid pressure. High confining pressure, high strain rates, low temperatures and high fluid pressures, all tend to lead to the propagation of cracks and flaws in rock and the development of brittle behaviour. High temperatures tend to produce deformation by plastic flow and creep.

The upper continental crust is generally made up of a skin of well stratified sedimentary and volcanic rocks usually less than 5 km in thickness. These sediments are generally porous and have a high fluid content; but the ease with which this fluid is able to migrate is often limited by variable permeability in different layers of the sedimentary pile.

This thin sediment skin usually lies on a more massive basement some 20–40 km in thickness usually consisting of granitic and gneissic rocks together with incorporated metasediments and metavolcanic materials. The properties of this basement are markedly different from those of the sedimentary cover. The basement generally shows a much less markedly layered structure, although it may possess a moderately strong anisotropic fabric (schistosity and gneissic banding). It usually has a much lower fluid content than the overlying sediments and the porosity and permeability are also lower. The deep basement is usually considered to be made up of dry rocks in the granulite facies. There is very good evidence to support the view

that an increase of heat in the deeper parts of orogenic areas enables the granitic rocks to become extremely ductile and locally to melt.

The deformation of continental crust at subduction zone sites is believed to give rise to the markedly linear orogenic zones such as the Alpine chains and Variscan and Caledonian deformation zones of northwest Europe and the Appalachians. It is not possible to observe the results of both the near surface and deep seated deformations at any one locality. But by taking samples of structural styles along a zone it is possible to see different erosion levels and to piece together a vertical view.

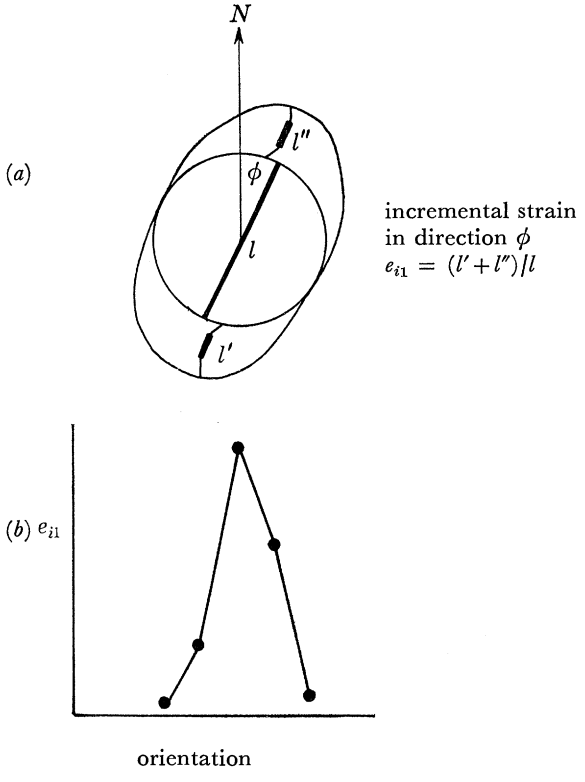

FIGURE 14. Method for calculating strain increments from the fibrous crystals in pressure shadow zones.

Deformation patterns in the uppermost volcano-sedimentary skin are controlled markedly by the layered nature of the rock. The strata are shortened and uplifted and the characteristic deformation styles are controlled by the development of buckle fold instabilities and by the production of fault discontinuities. The wavelengths of the folds are often fairly regular and are controlled by the thicknesses of the various stiffer or competent layers and by the contrast in ductility (μ) between the layers. High ductility contrasts and thick competent layers give rise to folds of longest wavelengths. The amplification rate of layers with high competence contrast (figure 15*a*) is large, whereas if the contrast in low, layer shortening takes place at a more marked rate than does fold amplification (figure 16). The fold styles are markedly controlled by the competence contrasts (cf. figures 15 and 16).

The strains in folded stratified material at a high tectonic level show a great range of orientation and value, but are systematically related to the position in the folds. Deformation fabrics resulting from strain (for example, slaty cleavage parallel to XY and linear structures parallel

to X) are also very variable in orientation and intensity (cf. figures 15 and 16). Ramberg has shown that under the influence of gravitational force the shortening rate is also an important factor controlling fold style and strain pattern, and that fold amplification is more rapid than layer shortening at high strain rates and vice versa at low strain rates. This implies that the finite strains (and associated rock fabrics) will be more homogeneous where the shortening rate is low.

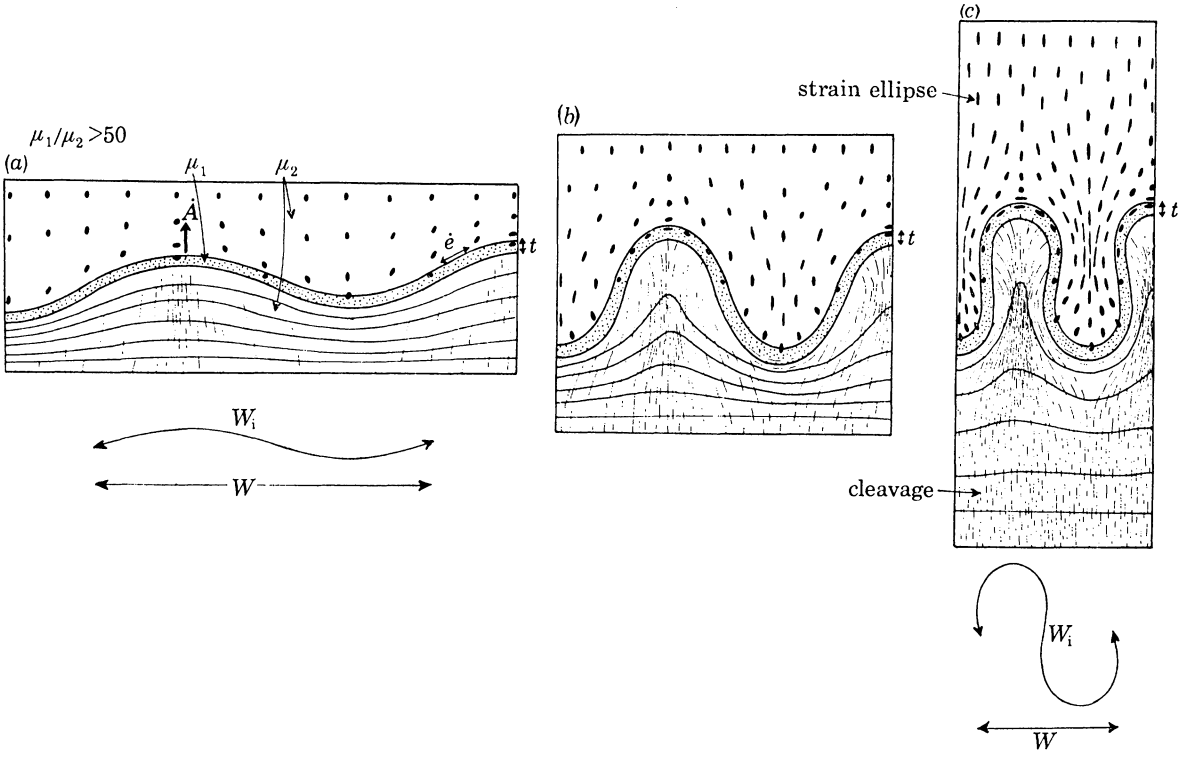

FIGURE 15. Strain developed around a folded single layer of stiff ductile material (ductility μ_1) embedded in a less competent host material (ductility μ_2). The layer shortening rate $\dot{e}$ is small compared with the fold amplification rate $\dot{A}$, and the initial wavelength W_i is large compared with the layer thickness ($> 12t$). W is the finite wavelength at particular stages in the finite evolution of the fold.

The abundance of pore water in the system is very important in controlling the deformation mechanism. Deformation of wet porous sediments by tectonic compaction closes up the pore spaces and high pore water pressure is built up. High fluid pressure leads to the development of tensile and shear failure and the development of detachment thrusts below impermeable horizons. Thin but extensive slabs of sediment become detached from their substratum and slide sideways under the influence of gravity. These nappes float like hovercraft on cushions of water being continuously fed by the underlying sediments undergoing dewatering. The abundance of fluid in the rocks also has a great effect on the chemical stability of individual crystals subject to differential stress. The process of pressure solution is particularly common in these zones. Material is removed from highly stressed sites and migrates by diffusion or flow in the fluid medium to become redeposited in pressure shadows and vein openings. The upper volcano-sedimentary zone is always characterized by the super-abundance of vein fissures filled with materials of high solubility (quartz, calcite and at higher temperatures and slightly deeper levels, albite, chlorite, epidote, actinolite).

At lower levels in the sediment pile, and at the interface between cover and granitic basement, the fold styles and associated strain variations are generally strongly influenced by the instabilities developed at the major competent/incompetent rock interface. This interface often becomes folded into a cuspate form, the anticlines of upfolded basement being more rounded than the tightly pinched synclines of downfolded sediments. Strains are particularly high in the synclinal hinges close to the interface.

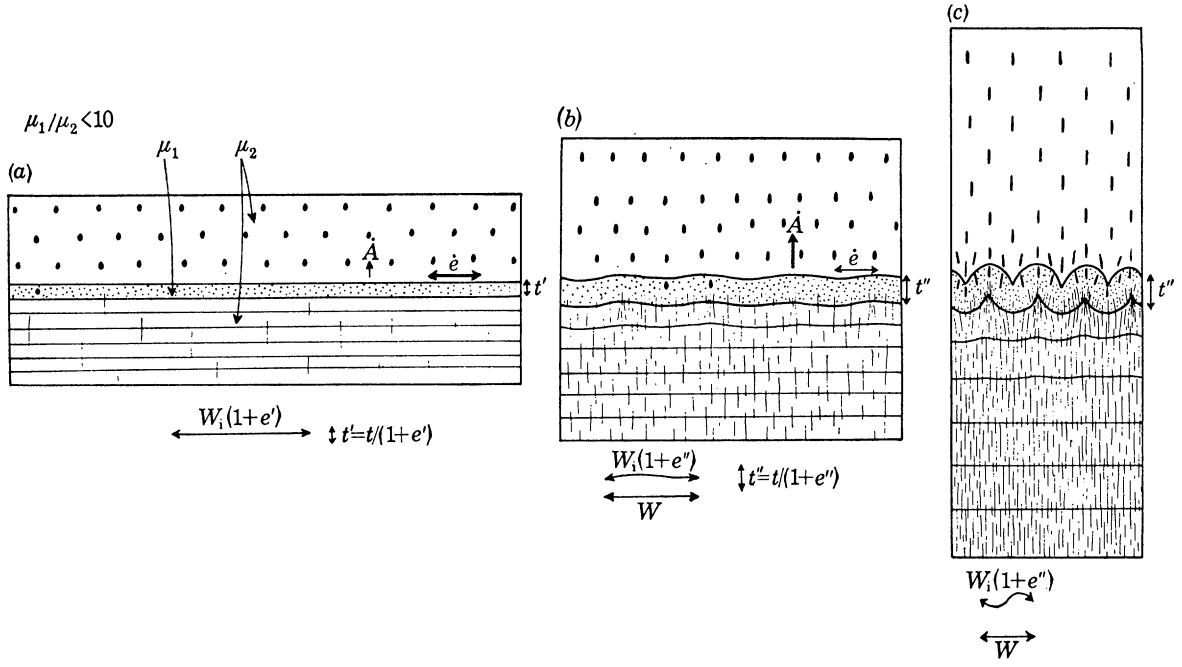

FIGURE 16. Strains developed around a single embedded competent layer where the competence contrast is low. Layer shortening is very important during the early stages of deformation and results in a marked increase in the thickness of the competent layer (initial t changes to t' and t''). Cf. with figure 15. (*a*) $\dot{A}$, amplification rate low; $\dot{e}$, layer shortening rate high; W_i, initial fold wavelength $< 8t$. (*b*) $\dot{A}$, accelerates; $\dot{e}$, decelerates.

The deformation of the basement proceeds in a quite different way to that in the cover. Its massive, generally non-layered structure, is not conducive to the types of buckling instability developed in the cover. Conjugate, semi-planar zones of high deformation known as shear zones are characteristic here. These deformation zones resemble ductile faults in that they enable relatively large scale differential displacements to occur in the blocks on either side of the zone. Shear zones in the Nagssugtoqidian orogenic belt in West Greenland (Escher *et al.* 1975) are many kilometres in width and take up a horizontal shortening of more than 60 %. Once a shear zone is initiated it appears to continue to develop by sideways propagation of its tip and probably by widening. The predominant effect seems to be that of strain softening in the rock and that once the basement has become deformed inside the zone, its ductility decreases. There are probably several reasons for this. The first is that the deformed material changes its properties by becoming highly anisotropic as planar and linear fabrics are built up in the zone (Ramsay & Graham 1970) and the second is that profound mineral changes generally take place in the shear zone as a result of a change of stability under new metamorphic conditions. These mineral and fabric changes are aided by water and alkali elements which tend to use the zone as a favoured channel for migration (Beach & Fyfe 1972). Much work still

needs to be done on the development of shear zones. It is still not certain what leads to their initiation – many probably grow from instabilities in the basement but some might arise by buckling instability at the cover – basement interface and propagate both upwards and downwards. In the Caledonian deformation zones of north Sutherland, it is possible to trace shear zones in the Lewisian basement upwards into the overturned limbs of folds in the Palaeozoic sediments of the cover. The strains in shear zones generally show a sigmoidal pattern of *XY* trajectory surfaces giving rise to an associated sigmoidal schistosity variation (figure 16) (Ramsay & Graham 1970).

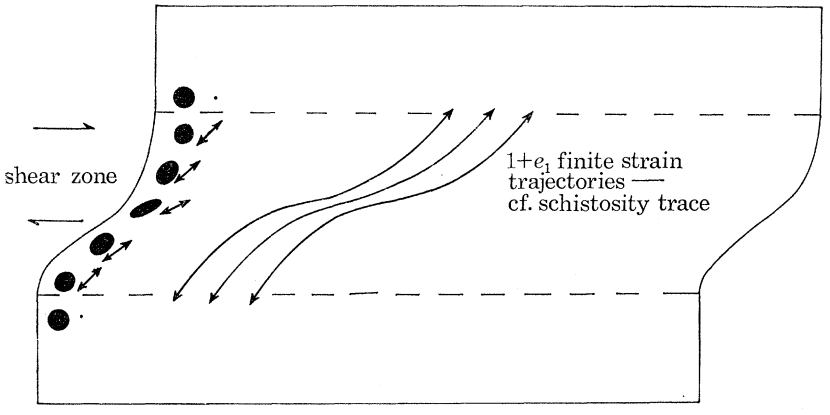

FIGURE 17. Characteristic strain pattern in a shear zone.

At the medium to deep crustal levels where shear zones develop, rock deformation generally proceeds by plastic flow processes. Pressure solution and cataclastic flow are inhibited by the dry conditions and high rock temperatures, and syn-deformational extension fracturing and vein development are rare.

Linear orogenic zones are characterized by multiple phases of deformation, particularly well developed in the central parts which crustal contraction is at a maximum value. The superimposed phases of deformation are separated by quiet periods during which the crust was either undergoing no displacement or undergoing uniform displacement. The thermal events which lead to the Barrovian type regional metamorphism in the internal zones usually reach their peak during one of the periods of deformation inactivity.

The styles of the late phases of deformation in regions of superimposed deformation are generally controlled by the mechanical instabilities developing in rocks which have previously acquired a strongly anisotropic fabric during early periods of deformation. These late deformations generally lead to the formation of kink folds, crenulation folds and internal boudinage (Cobbold *et al.* 1971). These late stage deformations often take place with pressure solution and vein forming processes, even though earlier deformations may have been accomplished by features more characteristic of plastic flow. It seems possible that the increase in metamorphic level and dehydration at depth can lead to rehydration of the relatively dry rocks at high tectonic levels.

CONCLUSIONS

The study of finite and progressive strain in naturally deformed rocks is one of the key techniques for the understanding of crustal deformation processes. Numerical evaluation of the strain state leads to an appreciation of the significance of large and small scale structural

phenomena, and summation of the strains enables the displacements across a deformed zone to be calculated. Computation of volumetric changes are sometimes possible and these help us to assess the importance of fluid and solid migration in the deformed rock system.

References (Ramsay)

Badoux, H. 1963 Les bélemnites tronçonnées de Leytron (Valais). *Bull. Lab. Geol. Lausanne* **138**, 1–7.

Barr, M. & Coward, M. P. 1974 A method for the measurement of volume change. *Geol. Mag.* **111**, 293–296.

Beach, A. & Fyfe, W. 1972 Fluid transport and shear zones at Scourie. *Contrib. Min. Pet.* **36**, 175–180.

Brace, W. F. 1961 Mohr construction in the analysis of large geological strain. *Bull. Geol. Soc. Am.* **72**, 1059–1080.

Brace, W. F. 1960 An analysis of large two dimensional strain in deformed rocks. *21 Int. Geol. Congr., Copenhagen* **18**, 261–269.

Breddin, H. 1964 Die tektonische Deformation der Fossilien und Gesteine in der Molasse von St. Gallen (Schweiz). *Geol. Mitt.* **4**, 1–68.

Cauchy, A. L. 1828 *Exercises de mathématique* **3**, 213–233.

Cloos, E. 1947 Oolite deformation in the South Mountain Fold, Maryland. *Bull Geol. Soc. Am.* **58**, 843–918.

Cobbold, P. R., Cosgrave, J. W. & Summers, J. M. 1971 Development of internal structures in deformed anistropic rocks. *Tectonophysics* **12**, 23–53.

Coward, M. P., James, P. R. & Wright, L. 1976 The movement pattern across the northern margin of the Limpopo mobile belt, Southern Africa. *Bull. Geol. Soc. Am.* (In the Press.)

Daubree, G. A. 1876 Expériences sur la schistosité des roches et sur les déformations des fossiles. *Compt. Rend. Acad. Sci. Paris.* **82**, 710–720.

Dunnet, D. 1969 A technique of finite strain analysis using elliptical particles. *Tectonophysics* **7**, 117–136.

Dunnet, D. & Siddans, A. W. B. 1971 Non-random sedimentary fabrics and their modification by strain. *Tectonophysics* **12**, 307–325.

Durney, D. W. & Ramsay, J. G. 1973 Incremental strains measured by syntectonic crystal growths. In *Gravity and tectonics* (ed. DeJong & Scholten), pp. 67–96. New York: Wiley & Sons Inc.

Elliott, D. 1970 Determination of finite strain and initial shape from deformed objects. *Bull. Geol. Soc. Am.* **81**, 2221–2236.

Elliott, D. 1972 Deformation paths in structural geology. *Geol. Soc. Am. Bull.* **83**, 2621–2638.

Escher, A., Escher, J. C. & Watterson, J. 1975 The reorientation of the Kangâmiut dyke swarm, West Greenland. *Can. J. Earth Sci.* **12**, 158–173.

Flinn, D. 1962 On folding during three dimensional progressive deformation. *Q. J. geol. Soc.* **118**, 385–433.

Gay, N. C. 1968 The motion of rigid particles embedded in a viscous fluid during pure shear deformation of the fluid. *Tectonophysics* **5**, 81–88.

Gay, N. C. 1969 The analysis of strain in the Barberton Mountain Land, Eastern Transvaal, using deformed pebbles. *J. Geol.* **77**, 377–396.

Haughton, S. 1856 On slaty cleavage and the distortion of fossils. *Phil. Mag.* **12**, 409–421.

Heim, A. 1878 *Untersuchungen über den Mechanismus der Gebirgsbildung*. Basel: Schwabe.

Heim, A. 1919 *Geologie der Schweiz*. Leipzig: Tauchnitz.

March, A. 1932 Mathematische Theorie der Regelungnach der Korngestalt. *Z. Krist.* **81**, 285–297.

Matthews, P. E., Bond, R. A. B. & van den Berg, J. J. 1974 An algebraic method of strain analysis using elliptical markers. *Tectonophysics* **24**, 31–67.

Owens, W. H. 1973 Strain modifications of angular density distributions. *Tectonophysics* **16**, 249–261.

Philips, J. 1843 On certain movements in the parts of stratified rocks. *Br. Ass. Adv. Sci.* 60–61.

Ramsay, J. G. 1967 *Folding and fracturing of rocks*. New York: McGraw Hill.

Ramsay, J. G. & Graham, R. H. 1970 Strain variation in shear belts. *Can. J. Earth Sci.* **7**, 786–813.

Ramsay, J. G. & Wood, D. S. 1973 The geometric effects of volume change during deformation processes. *Tectonophysics* **16**, 263–277.

Roberts, B. & Siddans, A. W. B. 1971 Fabric studies in the Llwyd Mawr ignimbrite. *Tectonophysics* **12**, 283–306.

Sharpe, D. 1846 On slaty cleavage. *Q. J. geol. Soc.* **3**, 74–105.

Sorby, H. C. 1855 On slaty cleavage as exhibited in the Devonian limestones of Devonshire. *Phil. Mag.* **11**, 20–37.

Talbot, C. J. 1970 The minimum strain ellipsoid using deformed quartz veins. *Tectonophysics* **9**, 47–76.

Tan, B. K. 1973 Determinations of strain ellipses from deformed ammonoids. *Tectonophysics* **16**, 89–101.

Wickham, J. S. & Elliott, D. 1970 Rotation and strain history in folded carbonates, Front Royal area, northern Virginia. *Trans. Am. Geophys. Union* **51**, 422.

PHILOSOPHICAL TRANSACTIONS OF THE ROYAL SOCIETY A MATHEMATICAL, PHYSICAL & ENGINEERING SCIENCES